Letter

^{16}O ^{16}O collisions at energies available at the BNL Relativistic Heavy Ion Collider and at the CERN Large Hadron Collider comparing α clustering versus substructure

Nicholas Summerfield,[1] Bing-Nan Lu,[2] Christopher Plumberg,[3] Dean Lee,[4] Jacquelyn Noronha-Hostler,[3] and Anthony Timmins[1]

[1]*Department of Physics, University of Houston, Houston, Texas 77204, USA*

[2]*China Academy of Engineering Physics, Graduate School, Building 8, No. 10 Xi'er Road, ZPark II, Haidian District, Beijing 100193, China*

[3]*Illinois Center for Advanced Studies of the Universe, Department of Physics, University of Illinois at Urbana-Champaign, Urbana, Illinois 61801, USA*

[4]*Facility for Rare Isotope Beams and Department of Physics and Astronomy, Michigan State University, East Lansing, Michigan 48824, USA*

(Received 13 March 2021; revised 12 July 2021; accepted 13 September 2021; published 4 October 2021)

Collisions of . light and heavy nuclei in relativistic heavy-ion collisions have been shown to be sensitive to nuclear structure. With a proposed ^{16}O ^{16}O run at the CERN Large Hadron Collider (LHC) and at the BNL Relativistic Heavy Ion Collider (RHIC) we study the potential for finding α clustering in ^{16}O. Here we use the state-of-the-art iEBE-VISHNU package with ^{16}O nucleonic configurations from *ab initio* nuclear lattice simulations. This setup was tuned using a Bayesian analysis on *p*Pb and PbPb systems. We find that the ^{16}O ^{16}O system always begins far from equilibrium and that at LHC and RHIC it approaches the regime of hydrodynamic applicability only at very late times. Finally, by taking ratios of flow harmonics we are able to find measurable differences between α-clustering, nucleonic, and subnucleonic degrees of freedom in the initial state.

DOI: 10.1103/PhysRevC.104.L041901

Introduction. In the past several years, the state of the art in the field of relativistic nuclear collisions has reached the threshold of precision physics [1–5]. The evolution of nuclear collisions is by now widely accepted to be well described within the framework of relativistic hydrodynamics, in which fluid dynamical behavior is manifested by a collective response to the initial collision geometry [6–14]. Precision measurements for probing the hydrodynamic evolution of nuclear collisions include a suite of flow observables [15,16], multiparticle correlation observables [17–19], soft-hard or heavy multiparticle azimuthal correlations [12,20–23], and femtoscopic radii [24–28], to name a few.

These observables are sensitive to the the initial state, the prehydrodynamic evolution [29–32], and the subsequent hydrodynamic phase. Essential to disentangling the effects of quantum fluctuations in the initial state and the prehydrodynamic evolution from those of the subsequent medium response is the ability to engineer initial conditions with specified geometries. This approach has been exploited already with great success in the context of small-system geometry engineering by the PHENIX Collaboration [33–40] and a quadruple deformation of ^{129}Xe was confirmed at the CERN Large Hadron Collider (LHC) [41–44]. More recently, dedicated runs of ^{16}O ^{16}O collisions have been proposed [22,45–51] at both the BNL Relativistic Heavy Ion Collider (RHIC) and LHC as a way of extending the geometry scan results to systems of intermediate size, which exhibit more exotic initial configurations due to an effect known as "α clustering."

The phenomenon of α clustering is a type of nucleon-nucleon (NN) correlation which is expected on the basis of nuclear lattice effective field theory (NLEFT) calculations to be present in doubly magic nuclei such as ^{16}O and ^{208}Pb. In such nuclei, nucleon positions are not completely uncorrelated, but tend to cluster together into groupings of two neutrons and two protons each, thereby effectively forming α particles (or "α clusters") in the nucleus. These correlations lead to quantifiable effects on the initial states of collisions between such nuclei and may manifest themselves in corresponding precision measurements of nuclear collision flow observables [49,52]. The possibility of measuring α clustering in ^{16}O is of enormous interest to the low-energy nuclear structure community [53–57]. It may also be possible to have subnucleonic fluctuations that would influence the collective flow [58–64]. A natural question is thus whether α clustering is measurable in relativistic heavy-ion collisions once all relevant effects have been considered.

The purpose of this paper is to explore the quantitative impact on flow observables of incorporating α clustering effects vs subnucleonic fluctuations into the initial conditions for hydrodynamic simulations of ^{16}O ^{16}O at both RHIC and LHC energies. To do this we adopt the state-of-the-art setup used in a recent Bayesian analysis [4] which was conditioned on experimental data at the LHC.

Initial conditions. Heavy ion collisions are rarely head on, but rather are characterized by a finite impact parameter. Consequently, a number of nucleons do not participate in the

TABLE I. Parameters from [74] for the Woods-Saxon density distribution used in the initial conditions.

	Parametrization	R (fm)	a (fm)	w (fm)
^{16}O	3pF	2.608	0.513	−0.051

collision, traveling on to the detector. Participating nucleons are counted using N_{part} and the impact region is treated as the initial condition for relativistic hydrodynamic calculations. In recent years [41,42,65–73] it has been found that the shape of the nucleus can play a role in the geometrical shape of the impact range, which is quantified through eccentricities. These eccentricities are connected to the collective flow observables through linear response for central [6–12] and mid-central collisions and linear+cubic response in peripheral collisions [1]. Thus, deformations in the shape of the nucleus are then translated to final state observables, which are most detectable in central collisions from linear response.

In order to model ^{16}O one uses a three-parameter fit [74] of the radial density distribution in the nuclear rest frame, written in spherical coordinates as

$$\rho(r,\theta,\phi) = \rho_0\left(1 + w\frac{r^2}{R^2}\right)\left[1 + \exp\left(\frac{r-R}{a}\right)\right]^{-1}, \quad (1)$$

with ρ_0 the nuclear saturation density, R a measure of the gluonic radius of the nucleus, and a the surface diffusion parameter. For nuclei such as ^{208}Pb, a "doubly magic" nucleus in the nuclear shell model, these spherically symmetric densities give a good description of elliptic flow at the LHC. The parameters used in our initial conditions are given in Table I. For ^{16}O, only the three-parameter fit (1) is available. Being a doubly magic nucleus, ^{16}O is taken to be spherically symmetric. We have coded this Woods-Saxon into the phenomenologically driven initial condition model, T$_{\rm R}$ENTo [68], using the following parameters: the thickness function scaling $p = 0$, the multiplicity fluctuations $k = 1.6$, and the nucleon width $\omega = 0.51$ fm. The nucleon-nucelon cross sections correspond to the p-p values at each energy investigated: $\sigma_{NN} = 42.5$ mb at $\sqrt{s_{NN}} = 200$ GeV (RHIC), and $\sigma_{NN} = 72.5$ mb at $\sqrt{s_{NN}} = 6.5$ TeV (LHC).

Ab initio structure and clustering. Nuclear clustering is a feature of many light nuclear systems and is particularly prevalent in nuclei with even and equal numbers of protons and neutrons. For such nuclei the clustering is mostly associated with the formation of α clusters. See, for example, Ref. [75] for a recent review. The nuclear states with the most pronounced α cluster substructures are excited states near α separation thresholds, such as the Hoyle state of ^{12}C. However the strong four-nucleon correlations also persist in ground states of nuclei. Recently it has even been suggested that the parameters of the nuclear force lie close to quantum phase transition between a nuclear liquid and a Bose gas of α particles [54].

One of the *ab initio* methods that is able to probe α clustering is nuclear lattice effective field theory (NLEFT). See Refs. [76,77] for reviews. In this work we use the nucleonic configurations for ^{16}O produced in Ref. [78]. These calculations used a simple leading order interaction, although the reproduction of the binding energies and radii of light and medium mass are accurate to a few percent error. In particular, the charge density distribution for ^{16}O is in excellent agreement with electron scattering data. These calculations were performed with a 1.32 fm spatial lattice spacing.

The nucleon configurations were computed using the pinhole algorithm introduced in Ref. [79]. The pinhole algorithm produces a classical distribution of the nucleon positions weighted according to the 16-nucleon density correlation function for the ^{16}O ground state. These 16-nucleon configurations provide the initial conditions for our hydrodynamics calculations to be described below. In the Supplemental Material [80], we quantify the amount of α clustering in the ^{16}O wave function. The short-range two-nucleon, three-nucleon, and four-nucleon correlations at lattice spacing 1.32 fm are only about 14% higher than that associated with a simple product state of four α clusters. Hence the degree of α clustering at the 1.32 fm distance scale is relatively high.

Hydrodynamic setup. We model the hydrodynamic evolution in ^{16}O ^{16}O using the Duke Bayesian tune of the iEBE-VISHNU package [4,64] to pPb and PbPb collisions at the LHC. The framework uses the T$_{\rm R}$ENTo model [68] to generate an initial entropy distribution. These distributions require normalization constants of 5.3 (RHIC) and 17 (LHC), which were obtained from an extrapolation of the energy dependence elsewhere [4]. The initial entropy distribution is then passed through a free-streaming phase of duration $\tau_s = 0.37$ fm/c and then used to initialize the hydrodynamic evolution at $\tau = \tau_s$. The construction of the hydrodynamic equation of state, as well as the temperature dependences of the specific bulk and shear viscosities $(\zeta/s)(T)$ and $(\eta/s)(T)$, are described in Ref. [64]. Finally, the hydrodynamic phase is terminated at a freeze-out temperature of $T_{fo} = 151$ MeV, at which point the system is converted to particles and evolved until kinetic freeze-out using ultrarelativistic quantum molecular dynamics (UrQMD) [81,82]. The final output is a collection of discrete particles at a final time step which may be used to compute observables of interest, such as flow coefficients and their ratios.

In order to make direct comparisons with experimental data, cumulants of the flow harmonics [17] are calculated usin:

$$v_n\{2\}^2 = \langle v_n^2 \rangle,$$
$$v_n\{4\}^4 = 2\langle v_n^2 \rangle^2 - \langle v_n^4 \rangle,$$

where the moments of the v_n distribution are used to calculate the cumulants. Centrality class bins are determined based on the initial state entropy density, which has been found to be a very good proxy for final state multiplicity distributions (used for experimental data). We have run 30 000 events for each different ion and configuration, and use subsampling to determine statistical error.

Results. Hydrodynamics is applicable when there is a large separation of scales. In relativistic heavy ion collisions there is some ambiguity of the correct scales to compare and, there-

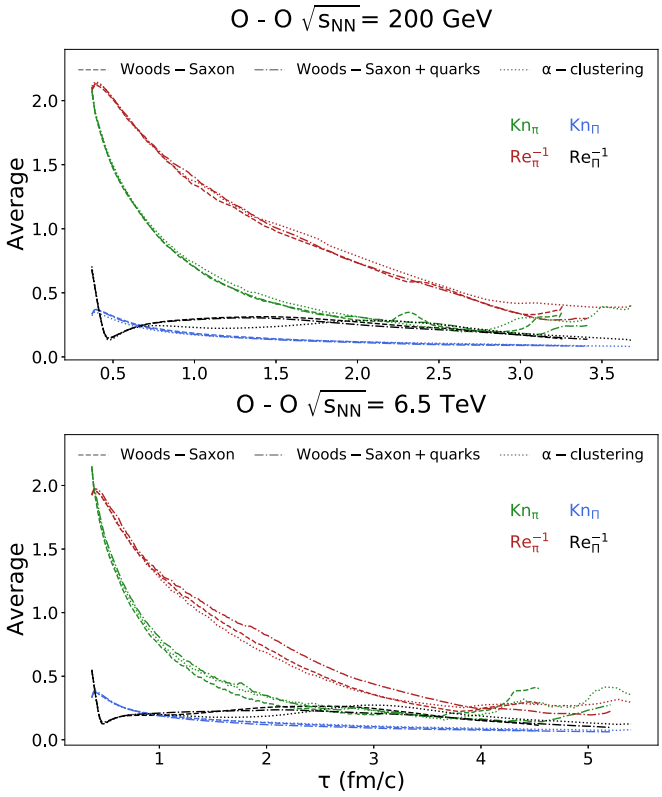

FIG. 1. Average Knudsen and inverse Reynolds values of regions above the freeze-out temperature (0.151 GeV) vs time for both $\sqrt{s_{NN}} = 200$ GeV (top) and $\sqrt{s_{NN}} = 6.5$ TeV (bottom) comparing the Woods-Saxon, Woods-Saxon + quarks, and α-clustering models with common initial conditions.

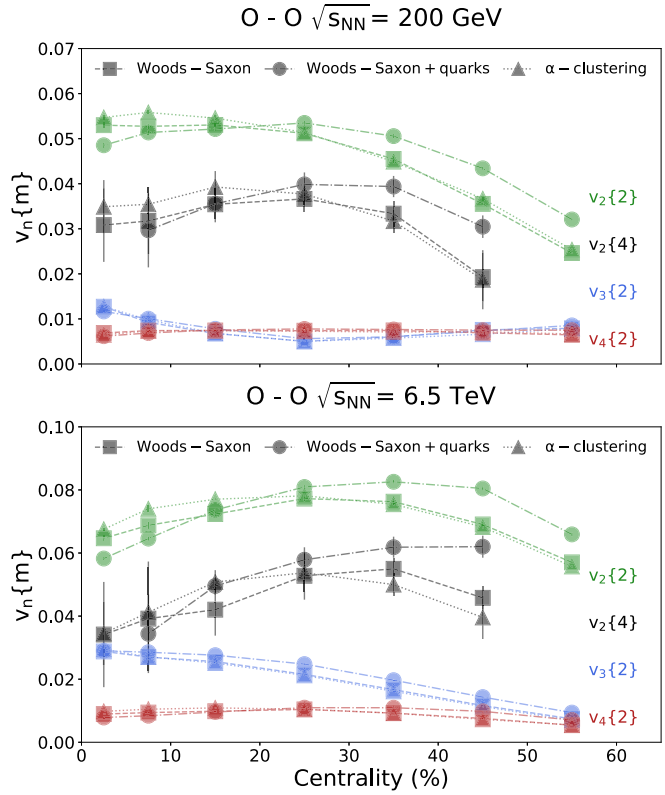

FIG. 2. Various flow coefficients ($v_n\{m\}$) vs centrality for both $\sqrt{s_{NN}} = 200$ GeV (top) and $\sqrt{s_{NN}} = 6.5$ TeV (bottom) comparing the Woods-Saxon, Woods-Saxon + quarks, and α-clustering models.

fore, multiple Knusden (Kn) and inverse Reynolds (Re^{-1}) numbers are used [83]:

$$\mathrm{Kn}_\pi = \tau_\pi \sqrt{\sigma_{\mu\nu}\sigma^{\mu\nu}}, \quad \mathrm{Re}_\pi^{-1} = \sqrt{\pi_{\mu\nu}\pi^{\mu\nu}}/P, \tag{2}$$

$$\mathrm{Kn}_\Pi = \tau_\Pi \theta, \quad \mathrm{Re}_\Pi^{-1} = |\Pi|/P. \tag{3}$$

We consider first in Fig. 1 the time evolution of the Kn and Re^{-1} numbers for bulk and shear, averaged at each time step over all fluid cells above the particlization temperature of $T_{\mathrm{switch}} = 0.151$ GeV for a single event (the same seed for the initial condition is chosen for Woods-Saxon, Woods-Saxon+substructure, and α clustering). We observe that, while the choice of initial-state model makes little difference to the time evolution of these quantities, both Kn$_\pi$ and Re$_\pi^{-1}$ are problematically large[1] ($\gtrsim$0.5) for the majority of the hydrodynamic phase, predominantly at early times $\tau \lesssim 2$ fm/c. This observation holds at both RHIC and LHC energies, and suggests that the hydrodynamic formalism is pressed to the limits of its validity in the description of intermediate systems such as ^{16}O ^{16}O . While Kn and Re^{-1} have been previously studied in an event averaged version of pPb [85], this is the first study of their values with the setup used within the Duke Bayesian analysis. It appears that eventually reasonable Kn and Re^{-1} are reached after $\tau \approx 3$ fm although there is some dependence on both the initial conditions. We note that one must consider the maximum of all Kn and Re^{-1} to determine the applicability of hydrodynamics and, therefore, these numbers indicate that even in intermediate systems one needs to consider the implications of far-from-equilibrium effects.

In Fig. 2 we present the flow cumulants predicted by our model at RHIC and LHC energies as functions of centrality, for the various initial-state models considered. We note that the largest quantitative effects are due to subnucleonic fluctuations and emerge at large centralities, while the effects of α clustering are somewhat smaller but on the same order of magnitude, and occur mainly at small centralities. v_2 is the most sensitive to details of the initial state, while v_3 and v_4 are only weakly affected. These features are expected from a hydrodynamic response to initial geometry which is dominated by fluctuations in central collisions and by global collision geometry in mid-central and peripheral collisions.

The effects of different ^{16}O ^{16}O initial-state models on the $v_m\{k\}$, although not qualitatively significant, should nevertheless be accessible for an analysis of $O(10^8)$ events collected in a short ^{16}O ^{16}O run at the LHC. Additional constraints can be obtained by considering ratios of flow coefficients as

[1]The choice in "large" as of yet unclear; others have chosen larger values, e.g., $\gtrsim$1 [84].

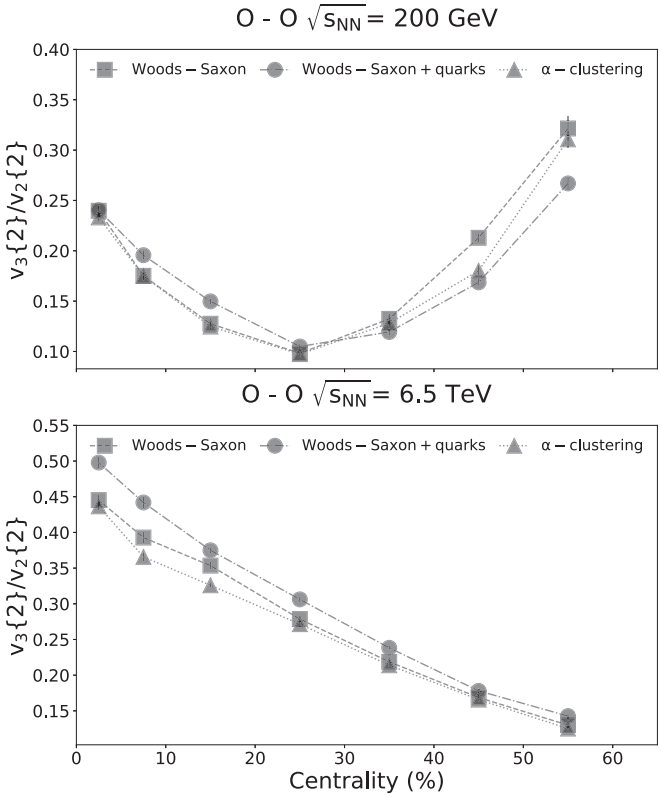

FIG. 3. $v_3\{2\}/v_2\{2\}$ vs centrality for both $\sqrt{s_{NN}} = 200$ GeV (top) and $\sqrt{s_{NN}} = 6.5$ TeV (bottom) comparing the Woods-Saxon, Woods-Saxon + quarks, and α-clustering models.

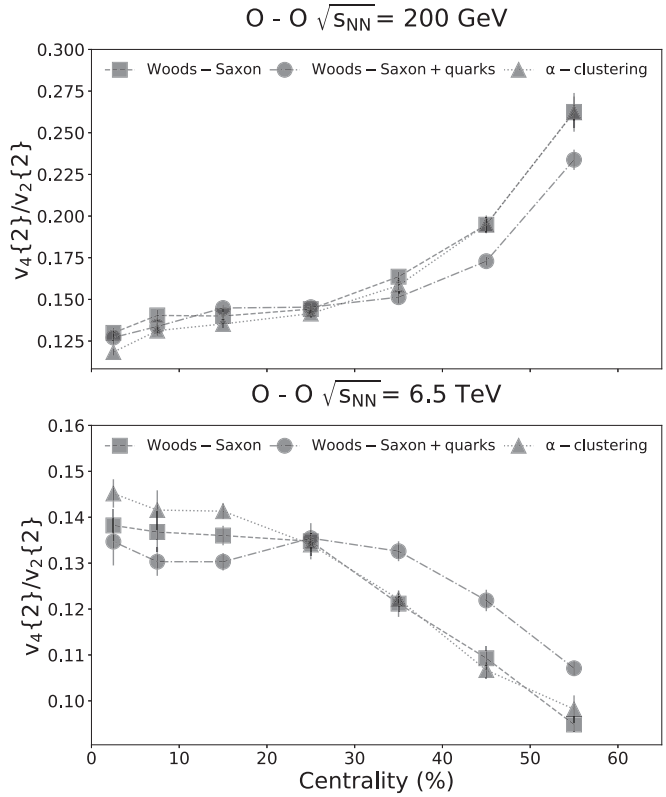

FIG. 4. $v_4\{2\}/v_2\{2\}$ vs centrality for both $\sqrt{s_{NN}} = 200$ GeV (top) and $\sqrt{s_{NN}} = 6.5$ TeV (bottom) comparing the Woods-Saxon, Woods-Saxon + quarks, and α-clustering models.

functions of centrality, as shown in Figs. 3–5. In this case, both subnucleonic fluctuations and α-clustering correlations lead to nontrivial and measurable effects. The ratio of $v_4\{2\}/v_2\{2\}$ shown in Fig. 3 demonstrates a suppression for α cluster in central collisions at the LHC, opposite to subnucleonic fluctuations that increase the ratio. This can be understood because α clustering enhances v_2 more than v_3. Perhaps the strongest effects are visible in the ratio $v_4\{2\}/v_2\{2\}$ (Fig. 4), where the effects of subnucleonic fluctuations and α clustering tend to act in opposite directions and may even produce detectable nonmonotonicity in the corresponding centrality dependences. This is especially important, given that the beam-energy dependence of the flow ratios contributes to the differences between RHIC and LHC energies in highly nontrivial ways. Quantitatively reproducing both the centrality and $\sqrt{s_{NN}}$ dependences of all flow ratios would therefore place stringent constraints on the importance of subnucleonic fluctuations and α clustering in real-world nuclear collisions, and provides motivation to carry out ^{16}O ^{16}O collisions at both RHIC and LHC energies.

Because v_4 appears to be the most promising observable to distinguish α clustering from subnucleonic fluctuations, we also study the quantity $v_4\{4\}^4$, which is sensitive to the fluctuations of v_4 on an event-by-event basis. $v_4\{4\}^4$ is a particularly interesting observable because hydrodynamic models have so far failed to capture its sign change at the LHC, even for well-understood PbPb collisions [86,87]. In Fig. 5 we find that at the LHC there is clear separation in $v_4\{4\}^4$ for central collision, which indicates a nice potential for distinguishing between α-clustering and subnucleonic fluctuations. Additionally, these mechanisms produce effects in opposite directions, with α clustering making $v_4\{4\}^4$ significantly more negative and subnucleonic fluctuations bringing the value of $v_4\{4\}^4$ close to 0. In contrast, RHIC does not provide a clear signal and it is unlikely that $v_4\{4\}^4$ could be used to distinguish between our three scenarios. Finally, we have also checked $v_2\{4\}/v_2\{2\}$ but found that all three initial conditions produced relatively similar results.

Conclusions. In this work we use *ab initio* lattice effective field theory calculations of the nuclear structure of ^{16}O coupled to the state-of-the-art relativistic hydrodynamics description of the quark gluon plasma to determine the possibility of measuring α clustering in relativistic heavy-ion collisions. We find that LHC energies are better suited to finding α clustering but one must consider ratios of harmonics such as $v_3\{2\}/v_2\{2\}$ and $v_4\{2\}/v_2\{2\}$. Interestingly enough, α clustering suppresses $v_3\{2\}/v_2\{2\}$ and enhances $v_4\{2\}/v_2\{2\}$ and in all our comparisons subnucleonic fluctuations always has the opposite effect compared to α clustering at LHC energies. Another promising observable is $v_4\{4\}^4$, where very significant differences appear between α clustering and subnucleonic fluctuations at 0–30% centrality at the LHC.

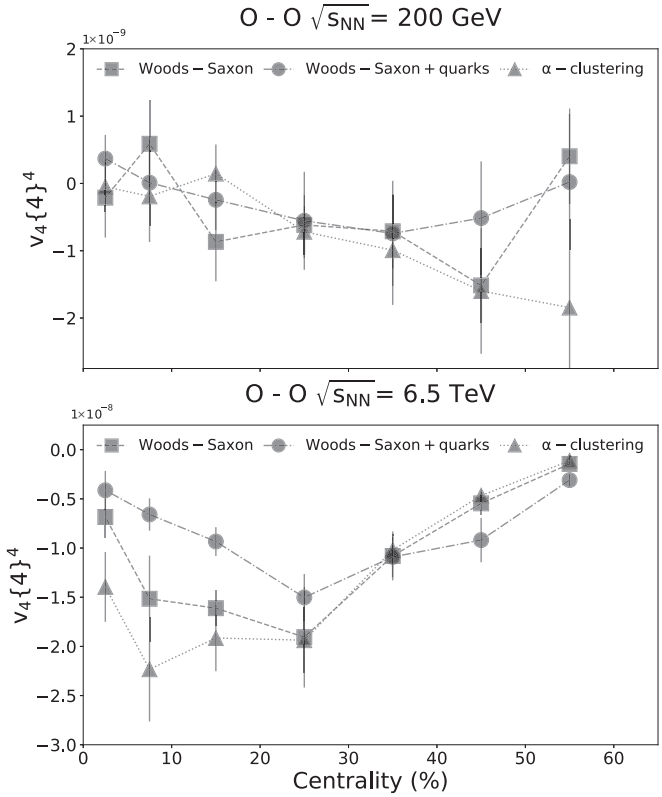

FIG. 5. $v_4\{4\}^4$ vs centrality for both $\sqrt{s_{NN}} = 200$ GeV (top) and $\sqrt{s_{NN}} = 6.5$ TeV (bottom) comparing the Woods-Saxon, Woods-Saxon + Quarks, and α clustering models.

In contrast, RHIC has more ambiguous results and appears less likely to be sensitive to α clustering but may be slightly sensitive to substructure.

While our results for Kn and Re^{-1} may be somewhat concerning, this does not immediately rule out the relativistic viscous hydrodynamics picture in small and intermediate systems. One possible solution may be anisotropic hydrodynamics [88–90], rederiving the hydrodynamic equations of motion in a far-from-equilibrium regime [91], effective transport coefficients [92–96], an intermediate stage between initial conditions and hydrodynamics [97,98], or even considering the Kn and Re^{-1} within the Bayesian analysis (and excluding parameter sets with unreasonable results). At the moment we do not look for attractors (originally proposed in [99]) in our simulations but leave that for a future work (complications arise in more realistic scenarios with shear and bulk coupled together and a realistic equation of state [100]).

Acknowledgments. The authors would like to thank Matthew Sievert for useful discussions related to this work. J.N.-H. and C.P. acknowledge the support from the U.S. DOE Nuclear Science Grant No. DE-SC0020633. D.L. acknowledges financial support from the U.S. Department of Energy (DE-SC0013365 and DE-SC0021152) and the NUCLEI SciDAC-4 Collaboration (DE-SC0018083) as well as computational resources from the Oak Ridge Leadership Computing Facility through the INCITE award "Ab-initio nuclear structure and nuclear reactions," the Jülich Supercomputing Centre at Forschungszentrum Jülich, RWTH Aachen, and Michigan State University. N.S. and A.T. were supported by DOE grant DE-FG02-07ER41521.

[1] J. Noronha-Hostler, L. Yan, F. G. Gardim, and J.-Y. Ollitrault, Linear and cubic response to the initial eccentricity in heavy-ion collisions, Phys. Rev. C **93**, 014909 (2016).
[2] H. Niemi, K. J. Eskola, R. Paatelainen, and K. Tuominen, Predictions for 5.023 TeV Pb+Pb collisions at the CERN Large Hadron Collider, Phys. Rev. C **93**, 014912 (2016).
[3] J. Adam *et al.* (ALICE Collaboration), Centrality Dependence of the Charged-Particle Multiplicity Density at Midrapidity in Pb-Pb Collisions at $\sqrt{s_{NN}} = 5.02$ TeV, Phys. Rev. Lett. **116**, 222302 (2016).
[4] J. E. Bernhard, J. S. Moreland, and S. A. Bass, Bayesian estimation of the specific shear and bulk viscosity of quark–gluon plasma, Nat. Phys. **15**, 1113 (2019).
[5] C. Shen and L. Yan, Recent development of hydrodynamic modeling in heavy-ion collisions, Nucl. Sci. Technol. **31**, 122 (2020).
[6] D. Teaney and L. Yan, Triangularity and dipole asymmetry in heavy ion collisions, Phys. Rev. C **83**, 064904 (2011).
[7] F. G. Gardim, F. Grassi, M. Luzum, and J.-Y. Ollitrault, Mapping the hydrodynamic response to the initial geometry in heavy-ion collisions, Phys. Rev. C **85**, 024908 (2012).
[8] H. Niemi, G. S. Denicol, H. Holopainen, and P. Huovinen, Event-by-event distributions of azimuthal asymmetries in ultrarelativistic heavy-ion collisions, Phys. Rev. C **87**, 054901 (2013).
[9] D. Teaney and L. Yan, Non linearities in the harmonic spectrum of heavy ion collisions with ideal and viscous hydrodynamics, Phys. Rev. C **86**, 044908 (2012).
[10] Z. Qiu and U. W. Heinz, Event-by-event shape and flow fluctuations of relativistic heavy-ion collision fireballs, Phys. Rev. C **84**, 024911 (2011).
[11] F. G. Gardim, J. Noronha-Hostler, M. Luzum, and F. Grassi, Effects of viscosity on the mapping of initial to final state in heavy ion collisions, Phys. Rev. C **91**, 034902 (2015).
[12] J. Noronha-Hostler, B. Betz, M. Gyulassy, M. Luzum, J. Noronha, I. Portillo, and C. Ratti, Cumulants and nonlinear response of high p_T harmonic flow at $\sqrt{s_{NN}} = 5.02$ TeV, Phys. Rev. C **95**, 044901 (2017).
[13] S. Rao, M. Sievert, and J. Noronha-Hostler, Baseline predictions of elliptic flow and fluctuations for the RHIC Beam Energy Scan using response coefficients, Phys. Rev. C **103**, 034910 (2021).
[14] M. Hippert, J. a. G. P. Barbon, D. Dobrigkeit Chinellato, M. Luzum, J. Noronha, T. Nunes da Silva, W. M. Serenone, and J. Takahashi, Probing the structure of the initial state of heavy-ion collisions with p_T-dependent flow fluctuations, Phys. Rev. C **102**, 064909 (2020).
[15] J. Schukraft, A. Timmins, and S. A. Voloshin, Ultra-relativistic nuclear collisions: Event shape engineering, Phys. Lett. B **719**, 394 (2013).

[16] S. Acharya *et al.* (ALICE Collaboration), Systematic studies of correlations between different order flow harmonics in Pb-Pb collisions at $\sqrt{s_{NN}} = 2.76$ TeV, Phys. Rev. C **97**, 024906 (2018).

[17] A. Bilandzic, R. Snellings, and S. Voloshin, Flow analysis with cumulants: Direct calculations, Phys. Rev. C **83**, 044913 (2011).

[18] M. Luzum and H. Petersen, Initial state fluctuations and final state correlations in relativistic heavy-ion collisions, J. Phys. G **41**, 063102 (2014).

[19] Y. Zhou, Review of anisotropic flow correlations in ultrarelativistic heavy-ion collisions, Adv. High Energy Phys. **2016**, 9365637 (2016).

[20] C. A. G. Prado, J. Noronha-Hostler, R. Katz, A. A. P. Suaide, J. Noronha, and M. G. Munhoz, Event-by-event correlations between soft hadrons and D^0 mesons in 5.02 TeV PbPb collisions at the CERN Large Hadron Collider, Phys. Rev. C **96**, 064903 (2017).

[21] S. Acharya *et al.* (ALICE Collaboration), Event-shape engineering for the D-meson elliptic flow in mid-central Pb-Pb collisions at $\sqrt{s_{NN}} = 5.02$ TeV, J. High Energy Phys. 02 (2019) 150.

[22] R. Katz, C. A. G. Prado, J. Noronha-Hostler, and A. A. P. Suaide, System-size scan of D meson R_{AA} and v_n using PbPb, XeXe, ArAr, and OO collisions at energies available at the CERN Large Hadron Collider, Phys. Rev. C **102**, 041901(R) (2020).

[23] CMS Collaboration Probing charm quark dynamics via multiparticle azimuthal correlations in 5.02 TeV PbPb collisions, CERN Technical Report No. CMS-PAS-HIN-20-001, 2021 (unpublished).

[24] A. Kisiel, W. Broniowski, M. Chojnacki, and W. Florkowski, Azimuthally-sensitive femtoscopy from RHIC to LHC in hydrodynamics with statistical hadronization, Phys. Rev. C **79**, 014902 (2009).

[25] L. Adamczyk *et al.* (STAR Collaboration), Beam-energy-dependent two-pion interferometry and the freeze-out eccentricity of pions measured in heavy ion collisions at the STAR detector, Phys. Rev. C **92**, 014904 (2015).

[26] A. Adare *et al.* (PHENIX Collaboration), Systematic study of charged-pion and kaon femtoscopy in Au+Au collisions at $\sqrt{s_{NN}} = 200$ GeV, Phys. Rev. C **92**, 034914 (2015).

[27] J. Adam *et al.* (ALICE Collaboration), Centrality dependence of pion freeze-out radii in Pb-Pb collisions at $\sqrt{s_{NN}} = 2.76$ TeV, Phys. Rev. C **93**, 024905 (2016).

[28] C. Plumberg, Hanbury-Brown–Twiss interferometry and collectivity in $p + p$, $p +$ Pb, and Pb + Pb collisions, Phys. Rev. C **102**, 054908 (2020).

[29] J. Liu, C. Shen, and U. Heinz, Pre-equilibrium evolution effects on heavy-ion collision observables, Phys. Rev. C **91**, 064906 (2015); [Erratum: **92**, 049904(E) (2015)].

[30] T.N. daSilva, D. Chinellato, G. S. Denicol, M. Hippert, M. Luzum, J. Noronha, W. Serenone, and J. Takahashi, Prehydrodynamic evolution and its signatures in final-state heavy-ion observables, Phys. Rev. C **103**, 054906 (2021).

[31] B. Schenke, C. Shen, and P. Tribedy, Hybrid color glass condensate and hydrodynamic description of the Relativistic Heavy Ion Collider small system scan, Phys. Lett. B **803**, 135322 (2020).

[32] G. Giacalone, B. Schenke, and C. Shen, Observable Signatures of Initial State Momentum Anisotropies in Nuclear Collisions, Phys. Rev. Lett. **125**, 192301 (2020).

[33] C. Aidala *et al.* (PHENIX Collaboration), Creation of quark–gluon plasma droplets with three distinct geometries, Nat. Phys. **15**, 214 (2019).

[34] A. Adare *et al.* (PHENIX Collaboration), Pseudorapidity Dependence of Particle Production and Elliptic Flow in Asymmetric Nuclear Collisions of $p +$ Al, $p +$ Au, $d +$ Au, and ^{3}He +Au at $\sqrt{s_{NN}} = 200$ GeV, Phys. Rev. Lett. **121**, 222301 (2018).

[35] A. Adare *et al.* (PHENIX Collaboration), Measurements of Elliptic and Triangular Flow in High-Multiplicity ^{3}He +Au Collisions at $\sqrt{s_{NN}} = 200$ GeV, Phys. Rev. Lett. **115**, 142301 (2015).

[36] C. Aidala *et al.* (PHENIX Collaboration), Measurement of long-range angular correlations and azimuthal anisotropies in high-multiplicity $p +$ Au collisions at $\sqrt{s_{NN}} = 200$ GeV, Phys. Rev. C **95**, 034910 (2017).

[37] A. Adare *et al.* (PHENIX Collaboration), Measurements of mass-dependent azimuthal anisotropy in central $p +$ Au, $d +$ Au, and ^{3}He +Au collisions at $\sqrt{s_{NN}} = 200$ GeV, Phys. Rev. C **97**, 064904 (2018).

[38] A. Adare *et al.* (PHENIX Collaboration), Measurement of emission angle anisotropy via long-range angular correlations with high p_T hadrons in $d +$ Au and $p + p$ collisions at $\sqrt{s_{NN}} = 200$ GeV, Phys. Rev. C **98**, 014912 (2018).

[39] C. Aidala *et al.* (PHENIX Collaboration), Measurements of azimuthal anisotropy and charged-particle multiplicity in $d +$ Au collisions at $\sqrt{s_{NN}} = 200$, 62.4, 39, and 19.6 GeV, Phys. Rev. C **96**, 064905 (2017).

[40] C. Aidala *et al.* (PHENIX Collaboration), Measurements of Multiparticle Correlations in $d +$ Au Collisions at 200, 62.4, 39, and 19.6 GeV and $p +$ Au Collisions at 200 GeV and Implications for Collective Behavior, Phys. Rev. Lett. **120**, 062302 (2018).

[41] G. Giacalone, J. Noronha-Hostler, M. Luzum, and J.-Y. Ollitrault, Hydrodynamic predictions for 5.44 TeV Xe+Xe collisions, Phys. Rev. C **97**, 034904 (2018).

[42] S. Acharya *et al.* (ALICE Collaboration), Anisotropic flow in Xe-Xe collisions at $\sqrt{\mathbf{s_{NN}}} = \mathbf{5.44}$ TeV, Phys. Lett. B **784**, 82 (2018).

[43] A. M. Sirunyan *et al.* (CMS Collaboration), Charged-particle angular correlations in XeXe collisions at $\sqrt{s_{NN}} = 5.44$ TeV, Phys. Rev. C **100**, 044902 (2019).

[44] G. Aad *et al.* (ATLAS Collaboration), Measurement of the azimuthal anisotropy of charged-particle production in Xe + Xe collisions at $\sqrt{s_{NN}} = 5.44$ TeV with the ATLAS detector, Phys. Rev. C **101**, 024906 (2020).

[45] Z. Citron *et al.*, Report from Working Group 5: Future physics opportunities for high-density QCD at the LHC with heavy-ion and proton beams, CERN Yellow Rep. Monogr. **7**, 1159 (2019).

[46] S. H. Lim, J. Carlson, C. Loizides, D. Lonardoni, J. E. Lynn, J. L. Nagle, J. D. Orjuela Koop, and J. Ouellette, Exploring new small system geometries in heavy ion collisions, Phys. Rev. C **99**, 044904 (2019).

[47] M. D. Sievert and J. Noronha-Hostler, CERN Large Hadron Collider system size scan predictions for PbPb, XeXe, ArAr, and OO with relativistic hydrodynamics, Phys. Rev. C **100**, 024904 (2019).

[48] S. Huang, Z. Chen, W. Li, and J. Jia, Disentangling contributions to small-system collectivity via scans of light nucleus-nucleus collisions, Phys. Rev. C **101**, 021901 (2020).

[49] M. Rybczyński and W. Broniowski, Glauber Monte Carlo predictions for ultrarelativistic collisions with ^{16}O, Phys. Rev. C **100**, 064912 (2019).

[50] A. Huss, A. Kurkela, A. Mazeliauskas, R. Paatelainen, W. van der Schee, and U. A. Wiedemann, Predicting parton energy loss in small collision systems, Phys. Rev. C **103**, 054903 (2021).

[51] B. Schenke, C. Shen, and P. Tribedy, Running the gamut of high energy nuclear collisions, Phys. Rev. C **102**, 044905 (2020).

[52] Y.-A. Li, S. Zhang, and Y.-G. Ma, Signatures of α-clustering in ^{16}O by using a multiphase transport model, Phys. Rev. C **102**, 054907 (2020).

[53] N. Furutachi, S. Oryu, M. Kimura, A. Dote, and Y. Kanada-En'yo, Cluster structures in oxygen isotopes, Prog. Theor. Phys. **119**, 403 (2008).

[54] S. Elhatisari, N. Li, A. Rokash, J. M. Alarcón, D. Du, N. Klein, B.-N. Lu, Ulf-G. Meißner, E. Epelbaum, H. Krebs, T. A. Lähde, D. Lee, and G. Rupak, Nuclear Binding Near a Quantum Phase Transition, Phys. Rev. Lett. **117**, 132501 (2016).

[55] R. Bijker and F. Iachello, The algebraic cluster model: Structure of ^{16}O, Nucl. Phys. A **957**, 154 (2017).

[56] L. Contessi, A. Lovato, F. Pederiva, A. Roggero, J. Kirscher, and U. van Kolck, Ground-state properties of ^{4}He and ^{16}O extrapolated from lattice QCD with pionless EFT, Phys. Lett. B **772**, 839 (2017).

[57] Y. Kanada-En'yo and D. Lee, Effective interactions between nuclear clusters, Phys. Rev. C **103**, 024318 (2021).

[58] J. S. Moreland, Z. Qiu, and U. W. Heinz, Imprinting quantum fluctuations on hydrodynamic initial conditions, Nucl. Phys. A **904-905**, 815c (2013).

[59] A. Dumitru, L. McLerran, and V. Skokov, Azimuthal asymmetries and the emergence of "collectivity" from multi-particle correlations in high-energy pA collisions, Phys. Lett. B **743**, 134 (2015).

[60] J. Noronha-Hostler, J. Noronha, and M. Gyulassy, Sensitivity of flow harmonics to subnucleon scale fluctuations in heavy ion collisions, Phys. Rev. C **93**, 024909 (2016).

[61] J. L. Albacete, H. Petersen, and A. Soto-Ontoso, Symmetric cumulants as a probe of the proton substructure at LHC energies, Phys. Lett. B **778**, 128 (2018).

[62] H. Mäntysaari, B. Schenke, C. Shen, and P. Tribedy, Imprints of fluctuating proton shapes on flow in proton-lead collisions at the LHC, Phys. Lett. B **772**, 681 (2017).

[63] F. G. Gardim, F. Grassi, P. Ishida, M. Luzum, P. S. Magalhães, and J. Noronha-Hostler, Sensitivity of observables to coarse-graining size in heavy-ion collisions, Phys. Rev. C **97**, 064919 (2018).

[64] J. S. Moreland, J. E. Bernhard, and S. A. Bass, Bayesian calibration of a hybrid nuclear collision model using p-Pb and Pb-Pb data at energies available at the CERN Large Hadron Collider, Phys. Rev. C **101**, 024911 (2020).

[65] W. Broniowski and E. Ruiz Arriola, Signatures of α Clustering in Light Nuclei from Relativistic Nuclear Collisions, Phys. Rev. Lett. **112**, 112501 (2014).

[66] L. Adamczyk *et al.* (STAR Collaboration), Azimuthal Anisotropy in U + U and Au + Au Collisions at RHIC, Phys. Rev. Lett. **115**, 222301 (2015).

[67] H. Wang and P. Sorensen (STAR Collaboration), Azimuthal anisotropy in U+U collisions at STAR, Nucl. Phys. A **932**, 169 (2014).

[68] J. S. Moreland, J. E. Bernhard, and S. A. Bass, Alternative ansatz to wounded nucleon and binary collision scaling in high-energy nuclear collisions, Phys. Rev. C **92**, 011901(R) (2015).

[69] A. Goldschmidt, Z. Qiu, C. Shen, and U. Heinz, Collision geometry and flow in uranium + uranium collisions, Phys. Rev. C **92**, 044903 (2015).

[70] M. Rybczyński, M. Piotrowska, and W. Broniowski, Signatures of α clustering in ultrarelativistic collisions with light nuclei, Phys. Rev. C **97**, 034912 (2018).

[71] B. Schenke, C. Shen, and P. Tribedy, Multi-particle and charge-dependent azimuthal correlations in heavy-ion collisions at the Relativistic Heavy-Ion Collider, Phys. Rev. C **99**, 044908 (2019).

[72] CMS Collaboration, Charged particle angular correlations in XeXe collision at $\sqrt{s_{NN}} = 5.44$ TeV, CERN Technical Report No. CMS-PAS-HIN-18-001, 2018 (unpublished).

[73] ATLAS Collaboration, Measurement of the azimuthal anisotropy of charged particle production in Xe+Xe collisions at $\sqrt{s_{NN}} = 5.44$ TeV with the ATLAS detector, CERN Technical Report No. ATLAS-CONF-2018-011, 2018 (unpublished).

[74] H. De Vries, C. W. De Jager, and C. De Vries, Nuclear charge and magnetization density distribution parameters from elastic electron scattering, At. Data Nucl. Data Tables **36**, 495 (1987).

[75] M. Freer, H. Horiuchi, Y. Kanada-En'yo, D. Lee, and Ulf-G. Meißner, Microscopic clustering in light nuclei, Rev. Mod. Phys. **90**, 035004 (2018).

[76] D. Lee, Lattice simulations for few- and many-body systems, Prog. Part. Nucl. Phys. **63**, 117 (2009).

[77] T. A. Lähde and U.-G. Meißner, *Nuclear Lattice Effective Field Theory: An introduction*, Lecture Notes in Physics Vol. 957 (Springer, Cham, 2019).

[78] B.-N. Lu, N. Li, S. Elhatisari, D. Lee, E. Epelbaum, and U.-G. Meißner, Essential elements for nuclear binding, Phys. Lett. B **797**, 134863 (2019).

[79] S. Elhatisari, E. Epelbaum, H. Krebs, T. A. Lähde, D. Lee, N. Li, B.-n. Lu, Ulf-G. Meißner, and G. Rupak, *Ab Initio* Calculations of the Isotopic Dependence of Nuclear Clustering, Phys. Rev. Lett. **119**, 222505 (2017).

[80] See Supplemental Material at http://link.aps.org/supplemental/10.1103/PhysRevC.104.L041901 for a more complete description of the methodology used here, including our approach to including α-clustering effects in the initial state and a more complete discussion of the sensitivity to α-clustering present in other nuclear collision observables, which includes Refs. [101–113].

[81] S. A. Bass *et al.*, Microscopic models for ultrarelativistic heavy ion collisions, Prog. Part. Nucl. Phys. **41**, 255 (1998).

[82] M. Bleicher *et al.*, Relativistic hadron hadron collisions in the ultrarelativistic quantum molecular dynamics model, J. Phys. G **25**, 1859 (1999).

[83] M. McNelis, D. Bazow, and U. Heinz, (3+1)-dimensional anisotropic fluid dynamics with a lattice QCD equation of state, Phys. Rev. C **97**, 054912 (2018).

[84] K. Gallmeister, H. Niemi, C. Greiner, and D. H. Rischke, Exploring the applicability of dissipative fluid dynamics to small systems by comparison to the Boltzmann equation, Phys. Rev. C **98**, 024912 (2018).
[85] H. Niemi and G. S. Denicol, How large is the Knudsen number reached in fluid dynamical simulations of ultrarelativistic heavy ion collisions? arXiv:1404.7327.
[86] G. Giacalone, L. Yan, J. Noronha-Hostler, and J.-Y. Ollitrault, The fluctuations of quadrangular flow, J. Phys.: Conf. Ser. **779**, 012064 (2017).
[87] P. Alba, V. Mantovani Sarti, J. Noronha, J. Noronha-Hostler, P. Parotto, I. Portillo Vazquez, and C. Ratti, Effect of the QCD equation of state and strange hadronic resonances on multiparticle correlations in heavy ion collisions, Phys. Rev. C **98**, 034909 (2018).
[88] W. Florkowski and R. Ryblewski, Highly-anisotropic and strongly-dissipative hydrodynamics for early stages of relativistic heavy-ion collisions, Phys. Rev. C **83**, 034907 (2011).
[89] M. Martinez and M. Strickland, Dissipative dynamics of highly anisotropic systems, Nucl. Phys. A **848**, 183 (2010).
[90] D. Bazow, U. W. Heinz, and M. Strickland, Second-order (2+1)-dimensional anisotropic hydrodynamics, Phys. Rev. C **90**, 054910 (2014).
[91] G. S. Denicol and J. Noronha, Fluid dynamics far-from-equilibrium: A concrete example, Nucl. Phys. A **1005**, 121996 (2021).
[92] P. Romatschke, Relativistic Fluid Dynamics Far From Local Equilibrium, Phys. Rev. Lett. **120**, 012301 (2018).
[93] J.-P. Blaizot and L. Yan, Fluid dynamics of out of equilibrium boost invariant plasmas, Phys. Lett. B **780**, 283 (2018).
[94] G. S. Denicol and J. Noronha, Hydrodynamic attractor and the fate of perturbative expansions in Gubser flow, Phys. Rev. D **99**, 116004 (2019).
[95] A. Behtash, S. Kamata, M. Martinez, and H. Shi, Dynamical systems and nonlinear transient rheology of the far-from-equilibrium Bjorken flow, Phys. Rev. D **99**, 116012 (2019).
[96] G. S. Denicol and J. Noronha, Connecting far-from-equilibrium hydrodynamics to resummed transport coefficients and attractors, Nucl. Phys. A **1005**, 121748 (2021).
[97] A. Kurkela, A. Mazeliauskas, J.-F. Paquet, S. Schlichting, and D. Teaney, Effective kinetic description of event-by-event pre-equilibrium dynamics in high-energy heavy-ion collisions, Phys. Rev. C **99**, 034910 (2019).
[98] A. Kurkela, A. Mazeliauskas, J.-F. Paquet, S. Schlichting, and D. Teaney, Matching the Nonequilibrium Initial Stage of Heavy Ion Collisions to Hydrodynamics with QCD Kinetic Theory, Phys. Rev. Lett. **122**, 122302 (2019).
[99] M. P. Heller and M. Spalinski, Hydrodynamics Beyond the Gradient Expansion: Resurgence and Resummation, Phys. Rev. Lett. **115**, 072501 (2015).
[100] T. Dore, J. Noronha-Hostler, and E. McLaughlin, Far-from-equilibrium search for the QCD critical point, Phys. Rev. D **102**, 074017 (2020).
[101] W. Zhao, Y. Zhou, K. Murase, and H. Song, Searching for small droplets of hydrodynamic fluid in proton–proton collisions at the LHC, Eur. Phys. J. C **80**, 846 (2020).
[102] D. Wertepny, J. Noronha-Hostler, M. Sievert, S. Rao, and N. Paladino, Ultracentral collisions of small and deformed systems at RHIC, Nucl. Phys. A **1005**, 121839 (2021).
[103] P. Carzon, S. Rao, M. Luzum, M. Sievert, and J. Noronha-Hostler, Possible octupole deformation of ^{208}Pb and the ultracentral v_2 to v_3 puzzle, Phys. Rev. C **102**, 054905 (2020).
[104] C. Gale, S. Jeon, B. Schenke, P. Tribedy, and R. Venugopalan, Event-by-Event Anisotropic Flow in Heavy-Ion Collisions from Combined Yang-Mills and Viscous Fluid Dynamics, Phys. Rev. Lett. **110**, 012302 (2013).
[105] H. Niemi, K. J. Eskola, and R. Paatelainen, Event-by-event fluctuations in a perturbative QCD + saturation + hydrodynamics model: Determining QCD matter shear viscosity in ultrarelativistic heavy-ion collisions, Phys. Rev. C **93**, 024907 (2016).
[106] J. L. Nagle and W. A. Zajc, Assessing saturation physics explanations of collectivity in small collision systems with the IP-Jazma model, Phys. Rev. C **99**, 054908 (2019).
[107] T. Lappi, Energy density of the glasma, Phys. Lett. B **643**, 11 (2006).
[108] G. Chen, R. J. Fries, J. I. Kapusta, and Y. Li, Early Time dynamics of gluon fields in high energy nuclear collisions, Phys. Rev. C **92**, 064912 (2015).
[109] P. Romatschke and U. Romatschke, *Relativistic Fluid Dynamics In and Out of Equilibrium*, Cambridge Monographs on Mathematical Physics (Cambridge University Press, Cambridge, 2019).
[110] T. Renk and H. Niemi, Constraints from v_2 fluctuations for the initial-state geometry of heavy-ion collisions, Phys. Rev. C **89**, 064907 (2014).
[111] G. Giacalone, J. Noronha-Hostler, and J.-Y. Ollitrault, Relative flow fluctuations as a probe of initial state fluctuations, Phys. Rev. C **95**, 054910 (2017).
[112] P. Carzon, M. D. Sievert, and J. Noronha-Hostler, Impact of multiplicity fluctuations on entropy scaling across system size, arXiv:2106.02525.
[113] R. Katz, C. A. G. Prado, J. Noronha-Hostler, J. Noronha, and A. A. P. Suaide, Sensitivity study with a D and B mesons modular simulation code of heavy flavor R_{AA} and azimuthal anisotropies based on beam energy, initial conditions, hadronization, and suppression mechanisms, Phys. Rev. C **102**, 024906 (2020).